A three-dimensional steady-state tumor system

Wenrui Hao[a,1], Jonathan D. Hauenstein[b,2], Bei Hu[a,*], Andrew J. Sommese[a,1]

[a] *Department of Applied and Computational Mathematics and Statistics, University of Notre Dame, Notre Dame, IN 46556*

[b] *Department of Mathematics, Mailstop 3368, Texas A&M University, College Station, TX 77843*

Abstract

The growth of tumors can be modeled as a free boundary problem involving partial differential equations. We consider one such model and compute steady-state solutions for this model. These solutions include radially symmetric solutions where the free boundary is a sphere and nonradially symmetric solutions. Linear and nonlinear stability for these solutions are determined numerically.

Keywords: Free boundary problems, stationary solution, stability, instability, bifurcation, discretization, condition number, Bertini, tumor growth.

1. The model

We consider the free boundary problem modeling tumor growth that was studied in [11; 12] and in the references [1; 3; 4; 5; 6; 7; 8; 9; 10; 13; 14; 15; 16].

Let $\Omega(t)$ denote the tumor domain at time t, and p the pressure within the tumor resulting from the proliferation of the tumor cells. The density of the cells, c, depends on the concentration of nutrients, σ, and, assuming that this dependence is linear, we simply identify c with σ. We also assume a linear dependence of the proliferation rate S on σ, namely $S = \mu(\sigma - \tilde{\sigma})$, where $\tilde{\sigma} > 0$ is a threshold concentration and μ is a parameter expressing the "intensity" of the expansion by mitosis (if $\sigma > \tilde{\sigma}$) or shrinkage by apoptosis (if $\sigma < \tilde{\sigma}$) within the tumor. The function σ satisfies the diffusion equation

$$\sigma_t - \Delta\sigma = -\sigma \qquad \text{in } \Omega(t). \tag{1}$$

The pressure p is related to the velocity $\vec{V}$ of the concentration σ, and, assuming Darcy's law in the tissue, we have $\vec{V} = -\nabla p$. Since, by conservation of mass, div $\vec{V} = S$, we obtain

*Corresponding author

Email addresses: whao@nd.edu (Wenrui Hao), jhauenst@math.tamu.edu (Jonathan D. Hauenstein), b1hu@nd.edu (Bei Hu), sommese@nd.edu (Andrew J. Sommese)

URL: www.math.tamu.edu/∼jhauenst (Jonathan D. Hauenstein), www.nd.edu/∼b1hu (Bei Hu), www.nd.edu/∼sommese (Andrew J. Sommese)

[1] This author was supported by the Duncan Chair of the University of Notre Dame and NSF grant DMS-0712910.

[2] This author was supported by Texas A&M University and NSF grant DMS-0915211.

that p satisfies the equation

$$\Delta p = -\mu(\sigma - \tilde{\sigma}) \qquad \text{in } \Omega(t). \tag{2}$$

As in the papers cited above, σ and p satisfy the boundary conditions

$$\sigma = 1 \qquad \text{on } \partial\Omega(t) \qquad (0 < \tilde{\sigma} < 1), \tag{3}$$

$$p = \kappa \qquad \text{on } \partial\Omega(t) \tag{4}$$

where κ is the mean curvature ($\kappa > 0$ if $\Omega(t)$ is a ball). Furthermore, the continuity condition $\vec{V} \cdot \vec{n} = V_n$ yields the relation

$$V_n = -\frac{\partial p}{\partial n} \qquad \text{on } \partial\Omega(t) \tag{5}$$

where n is the outward normal and V_n is the velocity of the free boundary $\partial\Omega(t)$ in the direction n. In summary, the model is the reaction-diffusion system

$$\begin{cases} \sigma_t - \Delta\sigma &= -\sigma & \text{in } \Omega(t) \\ -\Delta p &= \mu(\sigma - \widetilde{\sigma}) & \text{in } \Omega(t) \\ \sigma &= 1 & \text{on } \partial\Omega(t) \\ p &= \kappa & \text{on } \partial\Omega(t) \\ \frac{\partial p}{\partial n} &= -V_n & \text{on } \partial\Omega(t). \end{cases} \tag{6}$$

The steady-state tumor model of (6) is thus given by

$$\begin{cases} -\Delta\sigma &= -\sigma & \text{in } \Omega \\ -\Delta p &= \mu(\sigma - \widetilde{\sigma}) & \text{in } \Omega \\ \sigma &= 1 & \text{on } \partial\Omega \\ p &= \kappa & \text{on } \partial\Omega \\ \frac{\partial p}{\partial n} &= 0 & \text{on } \partial\Omega. \end{cases} \tag{7}$$

For the system (6) with smooth initial data, local existence and uniqueness was proven in [3]. In [13] it was proved that for any $0 < \tilde{\sigma} < 1$, there exists a unique radially symmetric stationary solution, and its radius depends on $\tilde{\sigma}$, but not on μ. Moreover, for small μ, the radially symmetric solutions are asymptotically stable. In [14], it was proved in the 2-dimensional case that there exists a sequence of symmetric-breaking branches of stationary solutions of (7) bifurcating from μ_n for $n = 2, 3, 4, \ldots$. A general simplified proof, which works also for the 3-dimensional case, was given in [10]. The asymptotic stability of the spherical solution for $\mu < \mu_2$ and of the first bifurcation branch was studied extensively in [11; 12] with earlier results for small μ established in [4].

These results imply, in particular, there exists a radially symmetric stationary solution with free boundary $r = R$ for any positive number R. Since tumors grown in vitro have a nearly spherical shape, it is important to determine whether these radially symmetric tumors are asymptotically stable.

While tumors grown in vitro have a nearly spherical shape, tumors grown in vivo are usually not. It is therefore also very interesting to study the behavior of nonradially symmetric tumors.

It was shown that the bifurcation points satisfy $\mu_2 < \mu_3 < \cdots$ and that it is possible for the radially symmetric solution to change stability at μ_2 [11]. Moreover, [12] showed that it is possible to have both a branch of stable and unstable nonradially symmetric solutions near μ_2. In particular, this shows that the nonradially symmetric solution branches near μ_2 are of particular interest.

We note that these results are valid only in a small neighborhood of the bifurcation branching point. A very challenging question is to find out what happens if the parameters *go beyond this small neighborhood.* It is clear that numerical computation is needed to answer these questions. In particular, it is interesting to find out whether it is possible for the tumor to grow into other shapes. This is the goal of this paper, by discretizing our system and tracking the condition number, we were able to track along the bifurcation branch well beyond the bifurcation point. In the process, we found a variety of possible shapes of steady state solutions. Some of these solutions are stable while some others are not. The solutions we obtained are shown in Figures 5–8. Moreover, it is remarkable that the bifurcation branches from μ_2 and μ_3 are crossed at a non-radial bifurcation shown in Figure 4.

2. Discretization

We utilize spherical coordinates to discretize the system with the exception of the origin and Z-axis, which are singular. Any spherical coordinate triplet (r, θ, ϕ), as shown in Figure 1, specifies a single point of three-dimensional space, namely

$$x = r\cos(\phi)\sin(\theta), \quad y = r\sin(\phi)\sin(\theta), \quad z = r\cos(\theta),$$

where

$$0 \le r < \infty, \quad 0 \le \theta \le \pi, \quad 0 \le \phi < 2\pi.$$

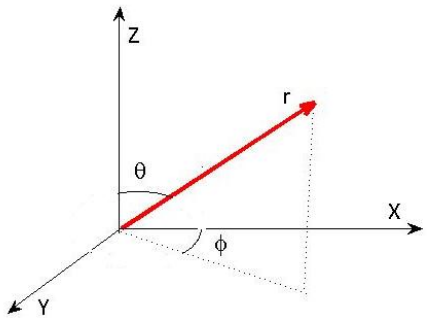

Figure 1: Spherical polar coordinates

We first consider the tumor model which is symmetrical in the ϕ direction. In this case, we just consider the model in the θ direction. We will discuss the model without such symmetry in Section 4. To handle the free boundary, we developed a novel discretization approach to allow the length of the grid to change in coordination with the boundary. That

is, let R_i be the length of tumor in the θ_i direction which changes independently and models the free boundary in this direction. In this case, we setup N_R equally spaced grid points between the origin and R_i in each direction. Let N_θ denote the number of grid points in the θ direction. Near the boundary, we add two additional grid points for improved accuracy that also change in accordance with the boundary. Figure 2 presents the grid points for a radial and nonradial solution with $N_\theta = 20$ and $N_R = 20$.

Table 1: Errors and orders

Formula	Value
$\max \lvert x_{10} - x_{20} \rvert$	7.94139×10^{-6}
$\max \lvert x_{10} - x_{40} \rvert$	7.41038×10^{-6}
$\max \lvert x_{20} - x_{40} \rvert$	6.08286×10^{-7}
$\max \lvert x_{10} - x_{80} \rvert$	7.36567×10^{-6}
$\max \lvert x_{20} - x_{80} \rvert$	6.55286×10^{-7}
$\max \lvert x_{40} - x_{80} \rvert$	4.48819×10^{-8}
$\log_2 \left(\frac{\lVert x_{10} - x_{80} \rVert_2}{\lVert x_{20} - x_{80} \rVert_2} \right)$	2.65067
$\log_2 \left(\frac{\lVert x_{20} - x_{80} \rVert_2}{\lVert x_{40} - x_{80} \rVert_2} \right)$	2.74774

Using this grid, we apply a third order finite difference scheme to setup a discretization of the system (7), which yields a polynomial system. The variables of this polynomial system correspond to the location of the boundary in each direction and the concentration of nutrients and pressure at each grid point. We checked the convergence of the numerical solution of the system by doubling and quadrupling the number of grid points. Table 1 shows that the numerical solution appears to be converging to the actual solution by increasing the number of grid points. In this table, x_j represents the solution with $N_R = N_\theta = j$ where $j = 10, 20, 40, 80$.

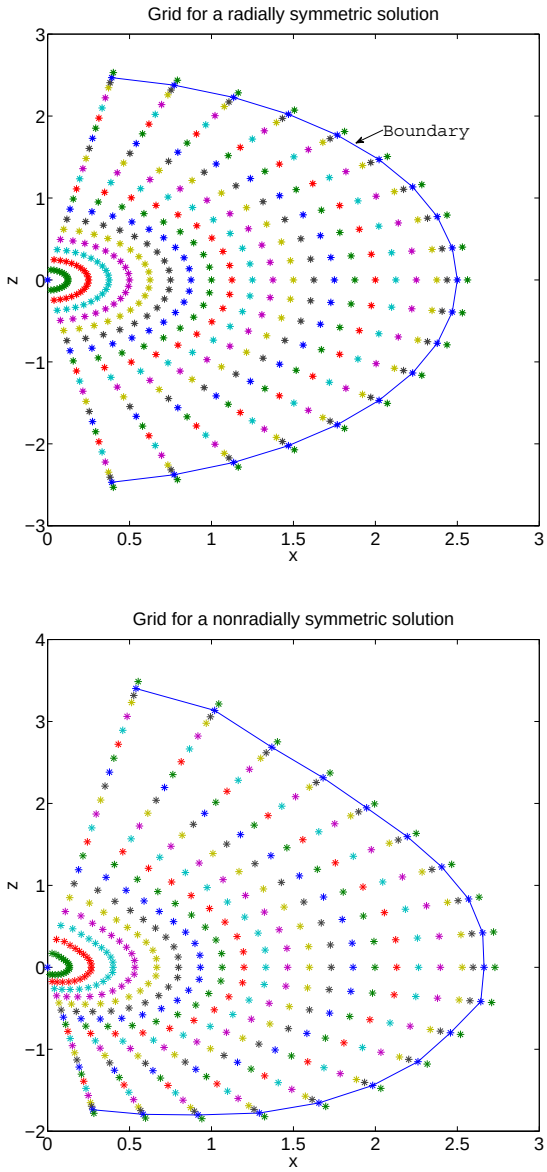

Figure 2: Grid points

3. Bifurcation problem

As mentioned in Section 1, the model depends on the positive parameter μ and, for a sequence of values $\mu_2 < \mu_3 < \cdots$, there exists branches of symmetry breaking stationary

solutions [10]. These solution branches extend beyond a small neighborhood of the bifurcation points which lie on the branch of radially symmetry solutions. One goal of this paper is to compute the values of μ_n where these bifurcations occur.

Starting from a radially symmetric solution and using parameter continuation with respect to μ, we tracked along the set of radially symmetric solutions of the discretized polynomial system for a given radius. At the values of μ where nonradially symmetric solution branches bifurcate, the radially symmetric solution is singular, that is, the Jacobian matrix of the non-symmetrized system is rank deficient. By monitoring the condition number, that is,

$$CN = \|J(x)\| \cdot \|J(x)^{-1}\| \tag{8}$$

where $J(x)$ is the Jacobian matrix of the discretized polynomial system evaluated at x, when performing parameter continuation, we can compute the values of $\mu_2, \mu_3, \ldots$ numerically. In our tests, the error between the numerically computed values of μ_n for $2 \leq n \leq 10$ and the theoretic values is relatively small. For example, using a radius of 2.5, we numerically computed $\mu_2 = 4.043$ and $\mu_3 = 9.314$. The theoretical values, rounded to three decimal places, are $\mu_2 = 4.042$ and $\mu_3 = 9.319$ [12]. Figure 3 plots the condition number with respect to μ as we track along the radially symmetric solution branch with radius 2.5 from $\mu = 3$ to $\mu = 10$. This plot clearly shows the increase in the condition numbers at μ_2 and μ_3.

In order to track along the multiple solution branches which intersect at μ_n, we numerically computed the tangent direction for each solution branch. Since the Jacobian matrix is singular at μ_n, we found that the double precision arithmetic in Matlab was unable to accurately compute these tangent directions. By using multiprecision arithmetic implemented in Bertini [2], we were able to compute the tangent directions which agreed with the symbolic formulas [12]. Upon computing the tangent direction, we utilized parameter continuation to track the nonradially symmetric solution branches passing through μ_2 and μ_3 which were computed above. Figure 4 shows the solution behavior of these branches which were computed using $N_R = N_\theta = 20$. For this figure, the function $\epsilon(\mu)$ is defined as the difference between $\max_\theta r(\theta, \mu)$ and $\min_\theta r(\theta, \mu)$. It is positive if $\min_\theta r(\theta, \mu)$ is reached first as θ goes from 0 to π and negative if $\max_\theta r(\theta, \mu)$ is reached first as θ goes from 0 to π , i.e.,

$$\epsilon(\mu) = (r(\overline{\theta}, \mu) - r(\underline{\theta}, \mu)), \tag{9}$$

where $\overline{\theta} \geq \underline{\theta}$ are value on which $\max_\theta r(\theta, \mu)$ and $\min_\theta r(\theta, \mu)$ are reached respectively. Figures 5–8 present a nonradially symmetric solution on each of these four nonradially symmetric solution branches displayed in Figure 4.

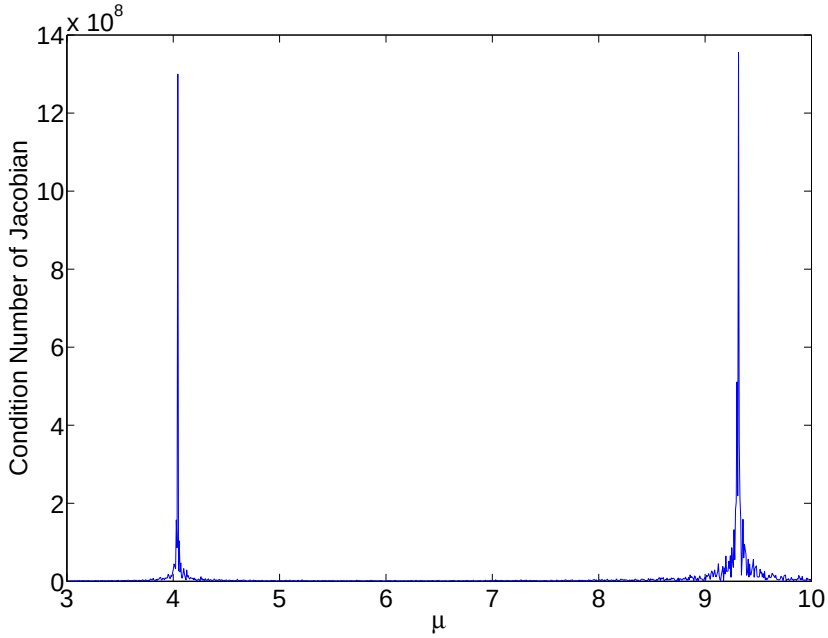

Figure 3: Condition Number Tracking

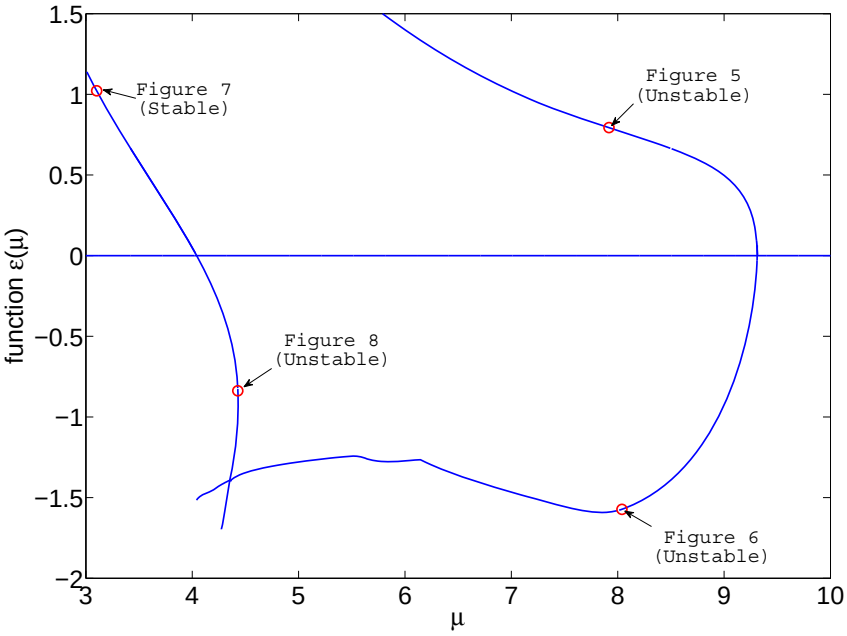

Figure 4: Solution Behavior

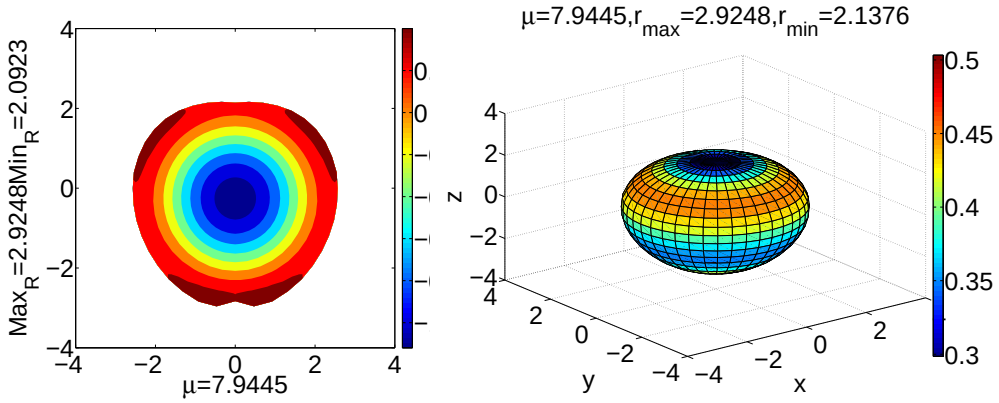

(a) Projection onto x, z plane (b) Three dimensional picture

Figure 5: $\mu = 7.9445$ on the upper branch

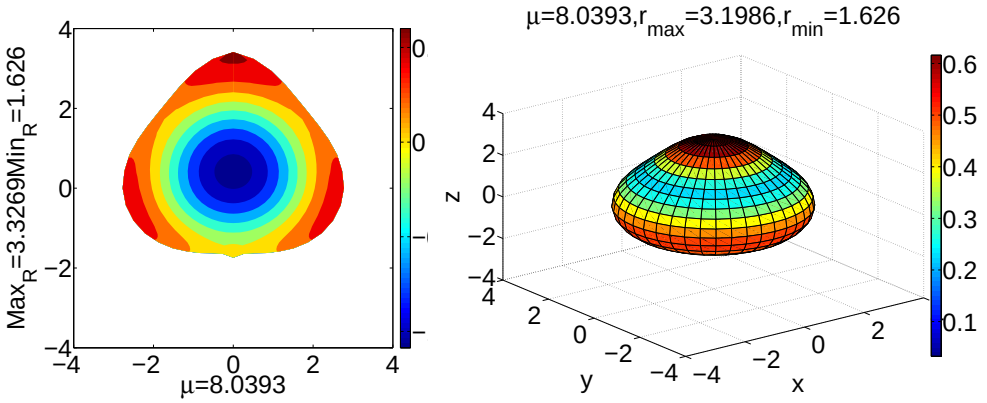

(a) Projection onto x, z plane (b) Three dimensional picture

Figure 6: $\mu = 8.0393$ on the lower branch

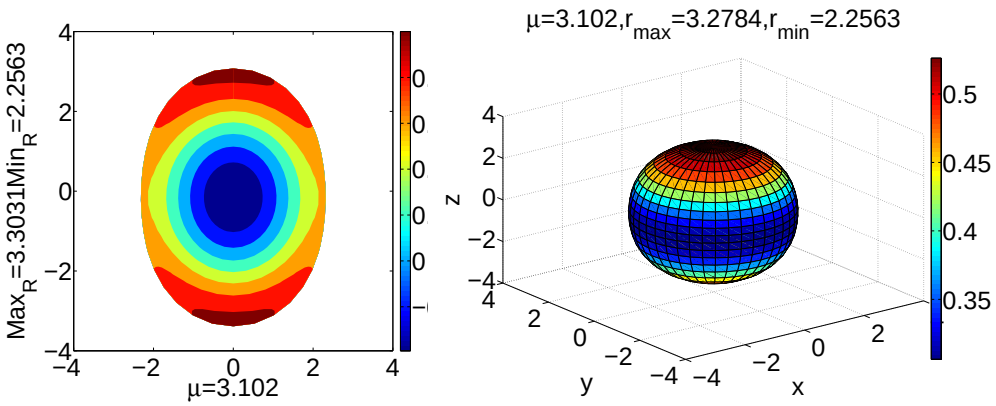

(a) Projection onto x, z plane (b) Three dimensional picture

Figure 7: $\mu = 3.102$ on the upper branch

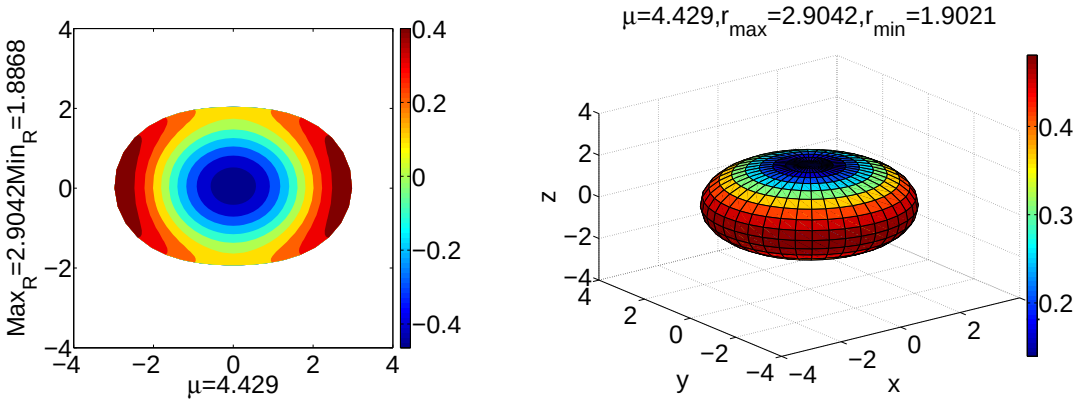

(a) Projection onto x, z plane

(b) Three dimensional picture

Figure 8: $\mu = 4.4291$ on the lower branch

4. The model without symmetry

It was shown in [12] that nonradial solutions near the bifurcation point μ_n has symmetry. We repeated our computation without imposing symmetry to look for other bifurcations. The left picture of Figure 9 shows the grid corresponding to a radially symmetric solution and the right picture of Figure 9 is the projection of the grid points onto the x, z plane.

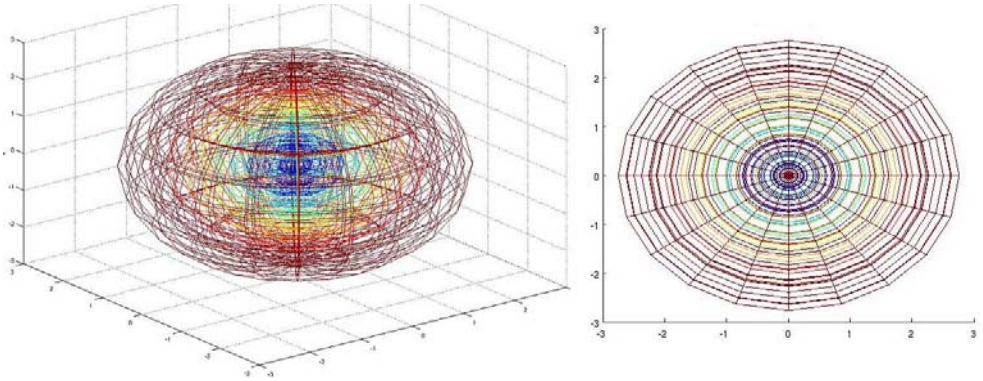

Figure 9: Grid points without symmetry

Since the system (7) is clearly translational and rotational invariant, upon removing the symmetry assumption, the system has five degrees of freedom from translations and rotations. The coordinates (x, y, z) of the origin yield the three degrees of freedom from translations with the rotations in θ and ϕ yielding the other two degrees of freedom. In particular, the resulting Jacobian of the discretized system has corank 5, which we verified numerically.

Since we are only concerned with families of solutions, we center the domain at the origin, fix the x-axis as parallel to the normal direction at $\theta = \pi/2, \phi = 0$, and fix the y-axis as parallel to the normal direction at $\theta = \pi/2, \phi = 3\pi/2$. With these choices, the Jacobian is full rank at solutions for generic μ. Moreover, the corank of this Jacobian is also 1 at the critical points of μ_2 and μ_3 and the nonradially solution branches are the same as obtained before. Additionally, we were unable to find any more bifurcation points by monitoring the condition number of the Jacobian along the radially symmetric solution branch.

5. Linear stability

The linearized system of (7), which is similar to the one computed in [17], is

$$\begin{cases} \sigma_{1t} - \Delta\sigma_1 + \sigma_1 = 0, & \text{in } \Omega_0 \\ -\Delta p_1 = \mu\sigma_1, & \text{in } \Omega_0 \\ \\ \sigma_1|_{r=\rho_0} = -\rho_1\sigma_{0r}|_{r=\rho_0}, \\ p_1|_{r=\rho_0} = \kappa_1 - \rho_1 \cdot p_{0r}\,|_{r=\rho_0}, \\ \rho_{1t}|_{r=\rho_0} = \left[\dfrac{p_{0r}\rho_{0\theta}}{\rho_0^2+\rho_{0\theta}^2} + \dfrac{p_{0\theta}}{\rho_0^2+\rho_{0\theta}^2}\right]\rho_{1\theta} + \left[\dfrac{p_{1\theta}\rho_{0\theta}}{\rho_0^2} - p_{1r}\right] \\ \qquad + \left[-\dfrac{p_{0r}\rho_{0\theta}^2}{\rho_0(\rho_0^2+\rho_{0\theta}^2)} - p_{0rr} + \dfrac{p_{0\theta r}\rho_{0\theta}}{\rho_0^2} - \dfrac{p_{0\theta}\rho_{0\theta}}{\rho_0^3} - \dfrac{p_{0\theta}\rho_{0\theta}}{\rho_0(\rho_0^2+\rho_{0\theta}^2)}\right]\rho_1. \end{cases} \tag{10}$$

Let τ denote the step size in time and $U^n = (\sigma_1(n\tau), p_1(n\tau), R_1(n\tau))$. Using a third order scheme in the spatial direction coupled with the backward Euler scheme in the time direction, which is unconditionally stable, we solve this linearized system. In particular, at each step in time, we solved the linear system $U^{n+1} = AU^n$, where the matrix A depends on σ_0, p_0, R_0, and τ.

This scheme transfers the question of linear stability to a question regarding the spectrum of the matrix A. In particular, if $|\rho(A)| < 1$, then $\|U^n\| \to 0$ which yields linear stability. Otherwise, it is linearly unstable. Tables 2 and 3 list the maximum absolute value of the eigenvalues of the matrix A for different values of μ along all the nonradially symmetric solution branches displayed in Figure 4. These tables show that $\max_{|\rho|}$ of the nonradially symmetric solutions are less than 1 when $\mu < \mu_2 \approx 4.042$ meaning that the nonradially symmetric solutions are linearly stable for $\mu < \mu_2$. For $\mu > \mu_2$, the nonradially symmetric solutions are unstable.

Table 2: Maximum eigenvalue for the "upper" branches in Figure 4

μ	$\max_{\lvert\rho\rvert}$	μ	$\max_{\lvert\rho\rvert}$	μ	$\max_{\lvert\rho\rvert}$
9.30460	1.0003895	8.49450	1.0003473	4.02897	0.9999995
9.22571	1.0003862	8.21950	1.0003308	3.92597	0.9999953
9.14521	1.0003825	7.94450	1.0003136	3.82297	0.9999911
9.06471	1.0003786	7.66950	1.0002958	3.71997	0.9999871
8.98421	1.0003745	7.39450	1.0002775	3.61697	0.9999834
8.90371	1.0003703	7.11950	1.0002589	3.51397	0.9999801
8.82321	1.0003660	6.84450	1.0002399	3.41097	0.9999773
8.74271	1.0003615	6.56950	1.0002206	3.30797	0.9999750
8.66221	1.0003570	6.29450	1.0002013	3.20497	0.9999732
8.58171	1.0003524	6.01950	1.0001824	3.10197	0.9999720

Table 3: Maximum eigenvalue for the "lower" branches in Figure 4

μ	$\max_{\lvert\rho\rvert}$	μ	$\max_{\lvert\rho\rvert}$	μ	$\max_{\lvert\rho\rvert}$
9.30996	1.0003897	7.99500	1.0002553	4.43128	1.0000753
9.21539	1.0003860	7.24500	1.0002989	4.43082	1.0000737
9.08177	1.0003776	6.49500	1.0003061	4.43169	1.0000745
8.94815	1.0003658	5.74500	1.0002070	4.39295	1.0000637
8.81453	1.0003514	4.99500	1.0002009	4.33595	1.0000521
8.68091	1.0003354	4.35318	1.0000877	4.27895	1.0000413
8.54729	1.0003185	4.38048	1.0000777	4.22195	1.0000309
8.41367	1.0003014	4.40151	1.0000771	4.16495	1.0000208
8.28005	1.0002846	4.41662	1.0000768	4.10795	1.0000111
8.14643	1.0002687	4.42651	1.0000762	4.05095	1.0000016

6. Nonlinear stability

We now turn our attention to determining nonlinear stability numerically. To that end, let $G := r - R(\theta, \phi) = 0$ be the equation describing the boundary. Then, the velocity V_n of $\partial\Omega(t)$ is

$$V_n = \frac{G_t}{\|\nabla G\|} = \frac{r_t r}{\sqrt{r^2 + R_\theta^2 + R_\phi^2/\sin(\theta)^2}}$$

Time marching with the system (6) allows one to numerically determine the local stability of the nonradial steady state solutions. This was accomplished by using a random perturbation of a nonradially-symmetric solution as the initial conditions for computing the steady-state solution. We used perturbations of the nonradially-symmetric solution of less than unit length. If the nonradial steady state solution is stable, the time marching solution will converge back to the unperturbed solution, otherwise, it will blow up.

For example, consider the solution corresponding to $\mu = 3.9422$ on the "upper" solution branch. Table 2 yields that this solution is linearly stable. We took a random pertubation, on the order of 10^{-3}, of this solution as the initial condition. Figure 10 shows the convergence of the perturbed solution back to the original solution when we perform time marching in t using (6). In particular, this shows that this nonradially symmetric solution is stable.

We performed similar computations to yield the stability of the solution branches which is displayed in Figure 11. In particular, green lines denote the stable solutions and red lines denote the unstable solutions. Therefore, we have numerically verified that the nonradially symmetric solutions are stable for $\mu < \mu_2$ and unstable for $\mu > \mu_2$.

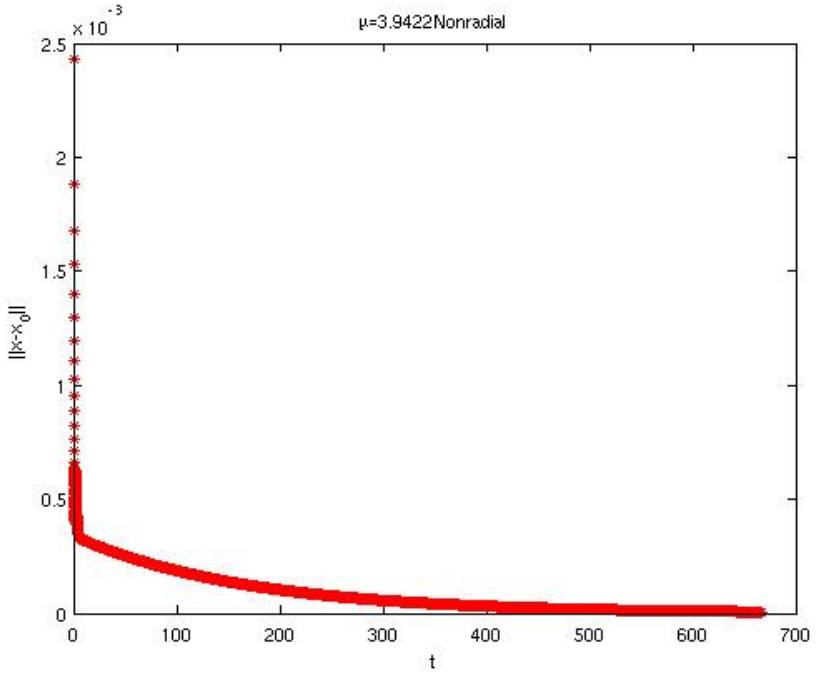

Figure 10: Convergence of the perturbed nonradially symmetric solution at $\mu = 3.9422$

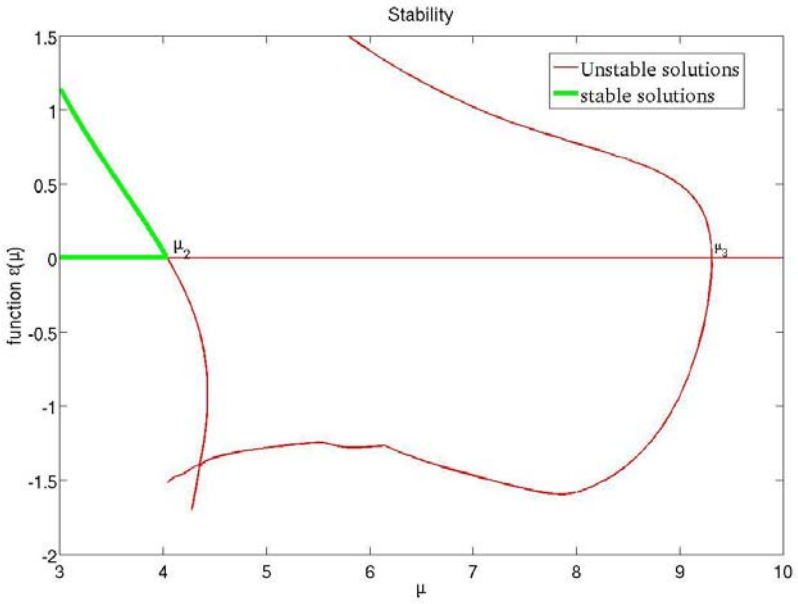

Figure 11: Stability of the solutions

References

[1] J.A. Adam, General aspect of modeling tumor growth and immune response, A Survey of Models for Tumor-Immune System Dynamics, edited by J.A. Adam and N. Bellomo, Birkhäuser, Boston, 14–87, (1996).

[2] D.J. Bates, J.D. Hauenstein, A.J. Sommese, and C.W. Wampler, Bertini: Software for numerical algebraic geometry. Available at www.nd.edu/∼sommese/bertini.

[3] B. Bazally and A. Friedman, A free boundary problem for elliptic-parabolic system: Application to a model of tumor growth, *Comm. Partial Diff. Eq.*, Vol 28, 517-560, (2003).

[4] B. Bazally and A. Friedman, Global existence and asymptotic stability for an elliptic-parabolic free boundary problem: an application to a model of tumor growth, *Indiana Univ. Math. J*, Vol 52, 1265–1304, (2003).

[5] N. Britton and M.A.J. Chaplain, A qualitative analysis of some models of tissue growth, *Math. Biosci.*, Vol 113, 77–89, (1993).

[6] H.M. Byrne, The importance of intercellular adhesion in the development of carcinomas, *IMA J. Math. Appl. Med. Biol.*, Vol 14, 305–323, (1997).

[7] H.M. Byrne, A weakly nonlinear analysis of a model of avascular solid tumor growth, *J. Math. Biol.*, Vol 39, 59–89, (1999).

[8] H.M. Byrne and M.A.J. Chaplain, Growth of nonnecrotic tumors in the presence and absence of inhibitors, *Math. Biosci.*, Vol 130, 151–181, (1995).

[9] H.M. Byrne and M.A.J. Chaplain, Modelling the role of cell-cell adhesion in the growth and development of carcinomas, *Mathl. Comput. Modelling*, Vol 12, 1–17, (1996).

[10] M. Fontelos and A. Friedman, Symmetry-breaking bifurcations of free boundary problems in three dimensions, *Asymptotic Analysis*, Vol 35, 187–206, (2003).

[11] A. Friedman and B. Hu, Bifurcation from stability to instability for a free boundary problem arising in a tumor model, *Arch. Rat. Mech. Anal.*, Vol 180, 293–330, (2006).

[12] A. Friedman and B. Hu, Stability and instability of Liapunov-Schmidt and Hopf bifurcation for a free boundary problem arising in a tumor model. *Trans. Amer. Math. Soc.*, Vol 360, 5291–5342, (2008).

[13] A. Friedman and F. Reitich, Analysis of a mathematical model for growth of tumor, *J. Math. Biology*, Vol 38, 262–284, (1999).

[14] A. Friedman and F. Reitich, Symmetry-breaking bifurcation of analytic solutions to free boundary problems: An application to a model of tumor growth, *Trans. Amer. Math. Soc.*, Vol 353, 1587–1634, (2000).

[15] H.P. Greenspan, Models for the growth of a solid tumor by diffusion, *Studies Appl. Math*, Vol 52, 317–340, (1972).

[16] H.P. Greenspan, On the growth of cell culture and solid tumors, *Theoretical Biology*, Vol 56, 229–242, (1976).

[17] W. Hao, J.D. Hauenstein, B. Hu, Y. Liu, A.J. Sommese, and Y.-T. Zhang Bifurcation of steady-state solutions for a tumor model with a necrotic core. Available at www.nd.edu/∼sommese/preprints.